Microscale Mapping of the Photon Detection Probability of SPADs

Eric Gros-Daillon[a], Loick Verger[a], Daniel A. B. Bonifacio[a,b], Edoardo Charbon[c], Claudio Bruschini[d], Leo Huf Campos Braga[c], Leonardo Gasparini[c], Nicola Massari[c], Matteo Perenzoni[c], David Stoppa[c], Robert. K. Henderson[f], Richard Walker[f], Ahmet Erdogan[f], Bruce Rae[g], Sara Pellegrini[g]

***Abstract*– A setup based on a microscope, a spectrograph and a servo positioning system is used to map the homogeneity of the PDP within SPADs, along the anode and the guard ring. Varying the wavelength of the incoming light enables to probe the device volume from the P-WELL to the N-WELL.**

I. INTRODUCTION

SINGLE-photon avalanche diodes (SPADs) realized in CMOS technology enable counting photons digitally, with on-chip implementation of advanced features such as active quenching and recharge, time-to-digital converters for multiple timestamping, triggering, etc. It is studied for a large field of applications including positron emission tomography, fluorescence lifetime imaging microscopy, and optical ranging. Photon detection probability (PDP) is a key feature of SPADs. In this work, we describe a method to map the SPAD PDP at a microscale level.

II. SETUP DESCRIPTION

The complete setup is composed by a microscope, a servo positioning controller, a spectrograph, a CCD camera and the SPAD data acquisition system, as shown in Fig. 1 (left).

A. The microscopic environment

A microscope (Olympus, Japan) has an objective with 100x amplification (numerical aperture 0.90, W. D. 1.0, F.N. 26.5). The microscope focuses a 1 µm FWHM light spot from the spectrograph into the SPAD sensitive surface. We utilized the SPAD array of the SPADnet-I sensor [1]. Light emitted by the NanoMetrics NanoSpec 9000i integrated film analysis system is collected by a focal length Czerny-Turner spectrograph type Shamrock SR303i-B by Andor technologies that disperses light into a frequency spectrum. The spectrograph has 303 mm focal length, F/4 aperture and 0.1 nm resolution. Andor software Solis was employed for wavelength selection and the control of the diffraction grating, The 1800 line/mm grating was used, because it gives the best resolution and a narrow spectral range coverage. Hence, the slit width was set to 20µm.

The SPAD data acquisition system is employed to perform photon counting procedures at a given position in the XY plane of the sensitive surface. A full scan in the surface is performed automatically using a servo positioning controller. For the scan, all light generated hits the SPAD.

Figure 1 (right) shows a typical image recorded by the CCD camera, which creates a small blue probe (center wavelength of 420 nm) onto the chip surface. The blue light spot is visible close to the center of the picture and can be compared to the 19.27 µm SPAD pitch. In this study, three center wavelengths were used : 420 nm to emulate the LYSO emission, 500 nm and 600 nm to investigate the PDP at several depths. The wavelength bandwith is around 50 nm. The incoming photon flux was kept far lower than the SPADs deadtime, which is 50 ns to avoid pile-up.

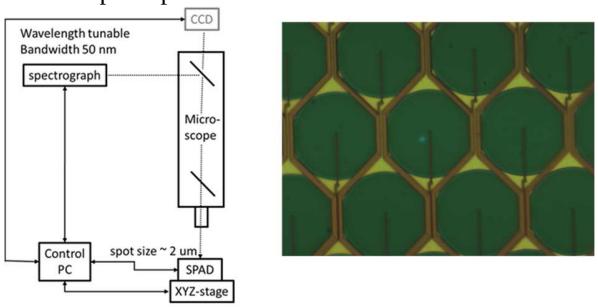

Fig. 1. Left: Measurement setup sketch. Right: image recorded by the microscope camera showing the SPADs and the blue spot.

B. The SPADnet-I chip

SPADnet-I is an 8×16 pixel array with 92,600 SPADs developed in 0.13-µm 1P4M CMOS front side illuminated (FSI) imaging technology from ST microelectronics which has been developed within the SPADnet consortium for PET applications. It is fully described in [1, 2] and characterized for spectrometric measurement in [3]. Only the features relevant for this study are summarized here. Each SPAD has a round shape to reduce dark count rate (DCR) and is organized in a

This work, conceived within the SPADnet project (www.spadnet.eu), has been supported by the European Community within the Seventh Framework Programme ICT Photonics and by the ENIAC JU Funded POLIS project.

a) Univ. Grenoble Alpes, F-38000 Grenoble, France. CEA LETI MINATEC Campus, F-38054 Grenoble France (e-mail: eric.grosdaillon@cea.fr).
b) Institute of Radioprotection and Dosimetry, IRD/CNEN, Rio de Janeiro, Brazil
c) Delft University of Technology, Delft, The Netherlands
d) EPFL, Lausanne, Swiss
e) Integrated Radiation and Image Sensors (IRIS), Fondazione Bruno Kessler, Trento, Italy
f) CMOS Sensors and Systems (CSS) Group, School of Engineering, the University of Edinburgh, Edinburgh, United Kingdom.
g) Imaging Division, STMicroelectronics, Edinburgh, United Kingdom

honeycomb structure, so as to enhance fill factor. Adjacent SPADs are placed in a single underlying deep N-well separated by an epi guard ring. The junction where the avalanche occurred is formed by a P-well implant. In order to reduce the total sensor DCR, noisy SPADs can be individually disabled using programmable memories.

C. *Acquisition environment*

The chip under test was mounted on a motorized translation stage. An evaluation kit for SPADnet-I is composed of a SP605 development board from Xilinx and a support board that enables to easily replace the chip under test. PC-based data acquisition and chip control are performed over Ethernet protocol using LabVIEW. The same PC controls the translation stage and enables to record the PDP map. For each acquisition position, the number of SPAD triggers (including real photons and dark counts) is recorded.

III. RESULTS

A. *PDP mapping*

For this study, groups of 3×3 SPADs were enabled. The chip was moved by steps of 1 µm. The integration time was fixed to 10 µs. The mean DCR was subtracted and the triggering rate was plotted versus the position, superimposed to the chip picture in Fig 2. The less than 1 µm width wires linked to the anodes are clearly resolved, showing a good spatial resolution. Around each sensitive area (red), there is a non-sensitive area (guard-ring), and a circular ring with reduced sensitivity (pale yellow).

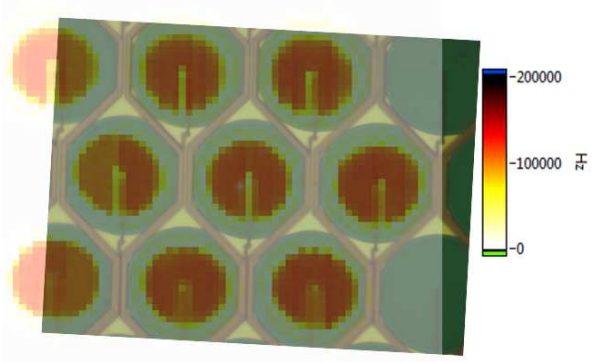

Fig. 2. Overlay of the PDP map onto the SPAD array picture.

B. *Variation with wavelength*

By changing the light wavelength, the triggering probability of the SPAD device can be investigated as a function of the depth of the triggering event. In this study, only a single SPAD was switched on. The absorption lengths of silicon for photons with wavelengths of 420 nm, 500nm and 600nm are 0.17µm, 0.75µm and 2.1µm, respectively. Increasing the wavelength, the interaction volume broadens. The anode wire is present only at the surface of the SPAD and can be easily noticeable in the profile only for the wavelength of 420 nm, which has higher absorption probability.

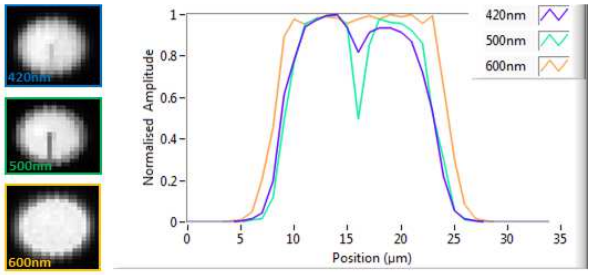

Fig. 3. Left: PDP map at three wavelengths. Right: horizontal cross sections.

IV. DISCUSSION

The obtained results could be compared to the electric field computed by technology computer-aided design (TCAD) [4]. The loss of efficiency around the edge of the SPAD is due to the implanted PWELL guard ring width around the P+ breakdown region and to the field curvature at the edge of the P+ region.

In the case of emissions at 420nm and 500nm, the absorption is very close to the surface, mainly electrons generated in the PWELL reach multiplication region. Some holes from the NWELL could also reach the multiplication region with a lower probability, thus creating the yellow halo.

At longer wavelengths, absorption reaches deeper silicon volume, holes created inside the NWELL region where they may be swept into the active region from a greater region of N around the SPAD.

V. CONCLUSION

A setup has been developed to map the PDP of SPADs at a microscale level. The comparison of this study to SPAD design and TCAD simulation of electric field will enable to estimate how much the p-well drawn area could be increased to optimize fill factor without causing the guard ring to fail.

By the time of the conference, more detailed results will be presented.

VI. ACKNOWLEDGMENTS

This work was supported by CNPq Brazilian agency.

REFERENCES

[1] L.H.C. Braga et al., “An 8x16-pixel 92k SPAD time-resolved sensor with on-pixel 64ps 12b TDC and 100MS/s real-time energy histogramming in 0.13um CIS technology for PET/MRI applications, digest of technical papers”, IEEE International Solid-State Circuits Conference, San Francisco, USA, 2013 pp 486-488.

[2] R. J. Walker, L. H. C. Braga, A. T. Erdogan, L. Gasparini, L. A. Grant, R. K. Henderson, N. Massari, M. Perenzoni, D. Stoppa, “A 92k SPAD Time-Resolved Sensor in 0.13µm CIS Technology for PET/MRI Application”, International Image Sensor Workshop, Utah USA, June 2013.

[3] E. Gros d’Aillon, L. Maingault, L. André, V. Reboud, L. Verger, E. Charbon, C. Bruschini, C. Veerappan, D. Stoppa, N. Massari, M. Perenzoni, L. H. C. Braga, L. Gasparini, R. K. Henderson, R. Walker, S. East, L. Grant, B. Jatekos, E. Lorincz, F. Ujhely, G. Erdei, P. Major, Z. Papp, and G. Nemeth, “First Characterization of the SPADnet sensor: a Digital Silicon Photomultiplier for PET Applications”, J. of Instr, 2013 JINST 8 C12026

[4] J. A. Richardson, E. A. G. Webster, L. A. Grant and R. K. Henderson, "Scaleable Single-Photon Avalanche Diode Structures in Nanometer CMOS Technology," in IEEE Transactions on Electron Devices, vol. 58, no. 7, pp. 2028-2035, July 2011.